Research Square

Preprints are preliminary reports that have not undergone peer review.
They should not be considered conclusive, used to inform clinical practice,
or referenced by the media as validated information.

Persistent insulin resistance is associated with adverse myocardial remodeling during left ventricular assist device support

Ke-Ying Pan
Nanjing Drum Tower Hospital
Er-Jun Zhu
First Affiliated Hospital of Harbin Medical University
Di-Hao Pan
First Affiliated Hospital Zhejiang University
Hai-Tao Zhang
Nanjing Drum Tower Hospital
Yong-Tao Li
First Affiliated Hospital of Harbin Medical University
Can Xu
Nanjing Drum Tower Hospital
Hui-Li Wang
Nanjing University of Chinese Medicine
Tong-Tong Zhu
Massachusetts General Hospital
Chang Liu
Nanjing Drum Tower Hospital
Jian Shi
Nanjing Drum Tower Hospital
Kun-Sheng Li
Nanjing Drum Tower Hospital
Hoshun Chong
Nanjing Drum Tower Hospital
Xi-Yu Zhu
Nanjing Drum Tower Hospital
Yun-Xing Xue
Nanjing Drum Tower Hospital
Gao-Jun Xu
Henan Provincial Chest Hospital
Shu-Min Wu

Henan Provincial Chest Hospital

Qiang Wang

Nanjing Drum Tower Hospital

Hao-Dong Pan

Ruijin Hospital

Dong-Jin Wang

Nanjing Drum Tower Hospital

Jason Z. Qu

Massachusetts General Hospital

Chun-Ling Yang

Nanjing Drum Tower Hospital

Tuo Pan

pan_tuo@126.com

Nanjing Drum Tower Hospital

Research Article

Keywords: Left ventricular assist device, Type 2 diabetes mellitus, Myocardial fibrosis, Soluble suppression of tumorigenicity-2

Posted Date: June 2nd, 2026

DOI: https://doi.org/10.21203/rs.3.rs-9739813/v1

License: This work is licensed under a Creative Commons Attribution 4.0 International License. Read Full License

Additional Declarations: No competing interests reported.

Abstract

Objective

Despite effective mechanical unloading, myocardial recovery after left ventricular assist device (LVAD) implantation remains highly heterogeneous. The determinants of this variable response, particularly the role of metabolic dysregulation during support, are incompletely understood.

Methods

In this multicenter, prospective cohort study, 54 consecutive patients (28 with type 2 diabetes mellitus (T2DM), 26 non-diabetic controls) undergoing LVAD implantation were followed longitudinally for up to 24 months. Serial assessments included the Triglyceride-Glucose (TyG) index (insulin resistance), soluble suppression of tumorigenicity-2 (sST2, fibrotic signaling), and left ventricular global longitudinal strain (LV-GLS, myocardial deformation). A surrogate composite fibrosis phenotype was defined by persistent elevation of sST2 (> 100 ng/mL at 6 and 12 months) combined with severely impaired LV-GLS (< 10% at 12 months).

Results

TyG remained elevated in T2DM during LVAD support (P<.001). No preoperative TyG-sST2 correlation, but significant positive association emerged from 6 months (all r > 0.50, P<.01) and persisted. LV-GLS recovery attenuated in T2DM vs. non-diabetics from 12 months. The surrogate composite fibrosis phenotype exclusively in T2DM (21.4% vs. 0%, P= .018).

Conclusion

Persistent insulin resistance during LVAD support is strongly associated with adverse remodeling, as characterized by delayed functional recovery and a surrogate fibrosis phenotype. These findings suggest that insulin resistance may represent a key therapeutic target beyond glycemic control in unloading-responsive myocardium, a hypothesis that warrants further investigation in prospective trials

INTRODUCTION

Left ventricular assist device (LVAD) implantation provides both lifesaving support and an opportunity for myocardial reverse remodeling in patients with advanced heart failure[1]. However, significant interindividual variability exists in the extent of structural and functional recovery following mechanical unloading[2]. This “responder” versus “non-responder” dichotomy remains a central challenge in optimizing post-LVAD outcomes[3].

A key biological substrate underlying this heterogeneous response is myocardial fibrosis. Persistent fibrosis after LVAD implantation is a recognized marker of limited reverse remodeling and adverse outcomes[4, 5]. In the clinical setting, directly and serially assessing myocardial fibrosis is challenging, driving the need for integrated surrogate markers that reflect both fibrotic stress and its functional consequences.

Beyond hemodynamic unloading, successful myocardial recovery is thought to require adaptive "metabolic reprogramming"[6, 7]. This places insulin resistance—a core defect in type 2 diabetes mellitus (T2DM)—at the center of a compelling clinical hypothesis. Insulin resistance may impair cardiac metabolic flexibility and promote a pro-fibrotic state through mechanisms that include the activation of the renin-angiotensin system (RAS), a pathway central to fibrosis in other diabetic complications [8–10], potentially limiting myocardial recovery even after LVAD unloading. However, current evidence is largely associative and fails to dynamically dissociate the effects of insulin resistance from those of hyperglycemia or the underlying ischemic substrate common in this population[11], impeding the development of targeted metabolic interventions[12].

To address this gap, we conducted a prospective, multicenter exploratory study to test the hypothesis that persistent insulin resistance during LVAD support is associated with an adverse remodeling phenotype characterized by impaired functional recovery and elevated fibrotic stress.. We investigated whether pre-existing T2DM and persistent insulin resistance are associated with adverse reverse remodeling and a fibrosis-predominant phenotype post-LVAD. By serially integrating the triglyceride-glucose (TyG) index (a marker of insulin resistance), soluble suppression of tumorigenicity-2 (sST2, a biomarker of fibrotic and inflammatory stress), and left ventricular global longitudinal strain (LV-GLS, a sensitive measure of systolic function), we aimed to characterize the dynamic interplay between metabolism and myocardial remodeling during LVAD support. We report a novel temporal observation: the association between insulin resistance and myocardial fibrotic stress appears to strengthen following LVAD implantation, offering a new perspective on the metabolic determinants of recovery heterogeneity.

MATERIALS AND METHODS

This was a multicenter, prospective, observational cohort study conducted between September 1, 2022, and December 31, 2025. The study protocol was approved by the Institutional Review Boards of all participating centers: Nanjing Drum Tower Hospital (Approval No. : 2024-577-02), The First Affiliated Hospital of Harbin Medical University (Approval No. : 202585), and The First Affiliated Hospital, Zhejiang University School of Medicine (Approval No.: IIT20250141B). Written informed consent was obtained from all participants or their legal guardians prior to enrollment. The study was conducted in accordance with the Declaration of Helsinki.

We consecutively screened 54 adult patients (aged ≥ 18 years) with end-stage heart failure who were scheduled to undergo implantation of a continuous-flow LVAD as either a bridge to transplantation or as

destination therapy. Patients were prospectively stratified into two groups based on the presence of T2DM or its absence (non-diabetic control group). The diagnosis of T2DM was strictly established according to the American Diabetes Association criteria prior to LVAD implantation.

Key exclusion criteria were applied to ensure cohort homogeneity and data integrity: 1) comorbidity-related exclusions: diagnosis of type 1 diabetes; acute myocardial infarction or stroke within 90 days prior to enrollment; active systemic infection or sepsis at the time of implantation; concomitant implantation of a right ventricular assist device (RVAD) or total artificial heart. 2) data integrity exclusions: inability to obtain high-quality echocardiographic images for reliable speckle-tracking analysis; anticipated inability to complete the core follow-up assessments with > 10% missing data for the study variables. 3) confounding condition exclusions: severe primary valvular heart disease requiring complex concomitant surgery other than routine repair; known infiltrative cardiomyopathy (e.g., amyloidosis, sarcoidosis).

Serial Clinical, Imaging, and Functional Assessment Protocol

All enrolled patients underwent a standardized prospective follow-up protocol with serial assessments scheduled pre-operatively (baseline) and at 3, 6, 12, and 24 months after LVAD implantation. Each visit included a structured clinical evaluation, venous blood sampling, comprehensive transthoracic echocardiography, and objective assessment of functional capacity.

Transthoracic echocardiography was performed at each time point by experienced cardiac sonographers using high-end ultrasound (GE Vivid E95 with cSound™) systems according to contemporary guidelines. Particular attention was paid to acquiring optimized grayscale images from standard parasternal and apical views to ensure clear endocardial border definition for subsequent speckle-tracking strain analysis. All echocardiographic data were transferred to a dedicated core laboratory for blinded offline analysis. To ensure the highest data quality and reproducibility, all quantitative measurements were performed independently by two experienced echocardiographers. Any discrepancies exceeding pre-defined acceptable limits—such as a difference greater than 5% for left ventricular ejection fraction (LVEF) or 1.5% for the absolute value of LV-GLS (|LV-GLS|)—were resolved through adjudication by a third senior investigator to establish a consensus value.

A comprehensive set of echocardiographic parameters was systematically quantified at every visit, as detailed in online supplement (eTable S1). This included conventional measures of left ventricular size and systolic function: left ventricular end-diastolic and end-systolic diameters (LVEDd, LVESd) and their ratio, measured from the parasternal long-axis view, and LVEF calculated via the biplane Simpson's method. Myocardial deformation was assessed by measuring left ventricular global longitudinal strain using speckle-tracking analysis on apical 4-, 2-, and 3-chamber views[13]. Following manual endocardial tracing, software tracked myocardial speckle patterns; segmental curves were reviewed and corrected as necessary. LV-GLS is reported as an absolute value (|LV-GLS|). Right ventricular systolic function was

evaluated using tricuspid annular plane systolic excursion (TAPSE), and pulmonary artery systolic pressure was estimated from the tricuspid regurgitation jet when feasible. LVAD-specific and advanced parameters were also assessed: aortic valve opening frequency (AVOF) was measured via pulsed-wave Doppler in the outflow graft, left ventricular geometry was characterized by the eccentricity index (EI) from a short-axis view, and right ventricular free-wall longitudinal strain (RVFWSL) was analyzed when image quality permitted.

Objective assessment of functional capacity included the standardized 6-minute walk test (6MWT) and symptom-limited cardiopulmonary exercise testing with breath-by-breath gas analysis for VO_2 max determination. For biomarker assessment, venous blood samples were collected and stored at -80°C. Soluble suppression of tumorigenicity-2 (sST2) levels were measured using a commercial Human ST2/Soluble ST2 ELISA Kit (XG-H1838, XG, Magnetic Particle Chemiluminescence Method), an assay specific for the soluble isoform. The precision of the sST2 assay was validated with intra- and inter-assay coefficients of variation < 5% and < 8%, respectively. Additionally, B-type natriuretic peptide (BNP) was quantified by a high-sensitivity immunoassay, and hemoglobin A1c (HbA1c) was analyzed for glycemic control evaluation. Insulin resistance was assessed using the Triglyceride-Glucose (TyG) index, calculated as Ln[fasting triglycerides (mg/dL) × fasting glucose (mg/dL) / 2][14].

Definition of LVAD-related significant myocardial fibrosis and clinical outcomes

In the absence of a universally accepted standard for quantifying myocardial fibrosis in patients supported by a LVAD, we developed a novel composite endpoint to identify significant, device-related pathological remodeling. This endpoint pragmatically integrates a circulating biomarker of myocardial fibrosis and mechanical stress, sST2 with a direct measure of myocardial contractile function, LV-GLS. The requirement for concordant and persistent abnormalities in both a molecular pathway and its functional consequence was designed to enhance diagnostic specificity and to capture a phenotype of "maladaptive fibrosis," where structural remodeling translates into sustained functional impairment. This approach aims to reduce misclassification from isolated, non-specific biomarker elevations (e.g., due to non-cardiac inflammation) or from imaging variability influenced by loading conditions. We emphasize that this is an exploratory, unvalidated operational definition intended for hypothesis generation in this specific cohort.

The derivation of thresholds for this composite endpoint was necessitated by the characteristics of the LVAD population. Previous studies have demonstrated that an sST2 level exceeding 28.8 ng/mL is associated with replacement myocardial fibrosis (RMF) in non-LVAD cohorts[15]. However, this threshold is not appropriate for our population, as patients undergoing LVAD implantation present with end-stage heart failure and extensive pre-existing fibrosis, evidenced by a reported median pre-implantation sST2 level of 74.2 ng/mL (IQR:54.7–116.9) that decreases significantly with unloading[16]. Robust evidence defining an optimal fibrosis-related cutoff in LVAD patients is lacking. Therefore, we established a

working threshold based on our own cohort data. Differences in sST2 between the T2DM and control groups emerged from 6 months post-implantation. The median sST2 levels for the entire cohort at 6, 12, and 24 months were 87.80 ng/mL (IQR:79.09–98.89), 77.65 ng/mL (IQR:68.10–89.13), and 59.01 ng/mL (IQR:42.53–67.03), respectively. Based on these distributions, we selected approximately 100 ng/mL (the upper quartile at 6 months) as a working cutoff reflecting significant myocardial fibrosis. Considering that 13 patients were lost to follow-up at 24 months, we required sST2 levels > 100 ng/mL at both 6 and 12 months to define persistent elevation, a criterion intended to minimize the confounding influence of transient perioperative inflammatory fluctuations and to capture a sustained signal potentially indicative of substantial myocardial fibrosis.

Similarly, for the functional criterion, we considered that standard LV-GLS cutoffs are derived from non-LVAD cohorts, where absolute LV-GLS (|LV-GLS|) > 18% reflects near-normal function and |LV-GLS| <14% indicates severe myocardial fibrosis[17]. In our study, differences in |LV-GLS| between groups appeared from 12 months post-implantation. The median |LV-GLS| for the entire cohort was 12% (IQR: 10–13%) at 12 months and 12% (IQR: 11–14%) at 24 months. Given the missing data at 24 months and to ensure high specificity for defining a group with unequivocally impaired function, we adopted a more stringent cutoff of |LV-GLS| <10% at 12 months as the functional criterion suggestive of significant myocardial fibrosis.

In summary, we combined both structural and functional markers to operationally define myocardial fibrosis. Patients were classified as having the fibrosis-dominant non-responder phenotype if they fulfilled all of the following criteria: (1) sST2 > 100 ng/mL at 6 months; (2) sST2 > 100 ng/mL at 12 months; and (3) |LV-GLS| <10% at 12 months. This composite binary classification, integrating a biomarker of sST2 with its LV-GLS, served as the pre-specified primary outcome and represents a pragmatic, albeit unvalidated against histology, operational definition for identifying high-risk patients in this clinical context.

Key secondary clinical outcomes were rigorously adjudicated by a blinded clinical endpoint committee using standardized definitions. These included all-cause mortality, heart failure re-admission (defined as an unplanned hospitalization requiring intravenous diuretic or inotropic therapy), stroke, LVAD-related infection (per International Society for Heart and Lung Transplantation criteria), and major gastrointestinal bleeding (clinically evident bleeding leading to hospitalization, transfusion, or a significant hemoglobin drop). Throughout the study, pharmacotherapy records were maintained, encompassing guideline-directed medical therapy for heart failure and antihyperglycemic agents in patients with type 2 diabetes mellitus, with adherence assessed via patient interview and prescription records.

Statistical Analysis

All statistical analyses were performed using SPSS (version 26.0, IBM Corp) and R (version 4.1.2), with a two-tailed P value < 0.05 considered statistically significant. Continuous variables are presented as

median with interquartile range (IQR) and compared using the Mann-Whitney U test, while categorical variables are presented as counts and percentages and compared using Fisher's exact test. These methods were applied for all cross-sectional comparisons between the T2DM and control groups across baseline characteristics, postoperative outcomes, and follow-up data. For post-hoc pairwise comparisons at individual time points derived from longitudinal models, a Bonferroni correction was applied to adjust for multiple testing.

To analyze longitudinal changes in serially measured parameters—including biomarkers (sST2, BNP), echocardiographic variables (|LV-GLS|, LVEF), Insulin resistance (TyG index), and functional capacity metrics (6MWT, VO_2 max)—we employed linear mixed-effects models[18]. These models accounted for within-subject correlations by incorporating a random intercept for each patient, with fixed effects for group (T2DM vs. Control), time, and their interaction. For time-to-event outcomes, Kaplan-Meier survival curves were constructed, and between-group differences were assessed using the log-rank test.

In the analysis stratified by myocardial fibrosis status (eTable S3), the non-parametric Mann-Whitney U test (denoted as †) and Fisher's exact test (denoted as ‡) were used to compare continuous and categorical variables, respectively, between the fibrosis and non-fibrosis groups, as indicated in the table footnote. Associations between continuous variables of interest were assessed using Spearman's rank correlation coefficient, with the correlation matrix visualized as a heatmap.

RESULTS

A total of 72 consecutive patients with end-stage heart failure scheduled for continuous-flow LVAD implantation were screened at three centers between September 2022 and December 2025. After applying exclusion criteria, 54 patients (median age 61.5 years, 92.6% male) were enrolled. The prevalence of pre-existing T2DM was high, both in the screened population (34/72, 47.2%) and the final cohort, where 28 patients (51.9%) constituted the T2DM group and 26 (48.1%) the non-diabetic control group. The groups were well-matched at baseline in terms of age, gender, body mass index, heart failure severity (NYHA class), and key echocardiographic/biomarker parameters including LVEF, |LV-GLS|, and preoperative sST2 levels (all $P > .05$; Table 1, eTable S1). As expected, baseline HbA1c, use of antihyperglycemic medications, and the Triglyceride-Glucose (TyG) index were all significantly higher in the T2DM group (all adjusted $P < .001$; eTable S1 in the online supplement).

To ensure comparisons under comparable mechanical unloading, LVAD operating parameters were compared throughout follow-up. No significant between-group differences were observed in speed, flow, or power at any postoperative time point (all $P > 0.05$; eTable S2 in the online supplement), confirming equivalent mechanical support and allowing direct assessment of T2DM's impact on myocardial response.

The composite endpoint of significant LVAD-related myocardial fibrosis occurred in T2DM patients (21.4% vs. 0%, $P = .018$). Longitudinal analyses revealed corresponding adverse remodeling trajectories

in the T2DM group, characterized by persistently higher sST2 levels from 6 months and significantly worse |LV-GLS| from 12 months onward (all between-group P < .05 at these time points; Fig. 1A, B). Linear mixed-effects modeling confirmed statistically significant main effects of both time and group, as well as a significant group-by-time interaction for sST2 (all P < 0.050). These results indicate that although sST2 levels declined progressively in both groups following mechanical unloading, the rate of decline was significantly attenuated in patients with T2DM. This divergent temporal pattern suggests that persistent insulin resistance sustains a pro-fibrotic milieu, thereby delaying the resolution of myocardial fibrotic stress—even in the presence of adequate hemodynamic unloading. For |LV-GLS|, only the main effect of time was significant (P < .001). Similarly, the TyG index was consistently higher in the T2DM group across all post-operative time points. Linear mixed-effects modeling confirmed a significant main effect of group (P<.001), indicating a sustained difference in insulin resistance status between T2DM and non-diabetic patients throughout the follow-up period. The group-by-time interaction was not significant (P=.245), suggesting parallel trajectories of change in both groups, albeit at different levels (Fig. 1C, eTable S1).

These adverse structural and metabolic trajectories paralleled impairments in functional capacity and cardiac geometry. Patients with T2DM demonstrated persistently lower functional capacity, evidenced by shorter 6-minute walk distances (main effect of group: P = .043; Fig. 1D) and lower peak VO_2 (main effect of group: P = .013; Fig. 1E). The left ventricular end-diastolic to end-systolic diameter ratio (LVEDd/LVESd) showed a significant difference in remodeling patterns between groups (group-by-time interaction: P = .007), and HbA1c remained worse in the T2DM group throughout the study (main effect of group: P < .001; Fig. 1F). No significant differences were found between groups in early postoperative outcomes, overall survival, or other major LVAD-related complications (Table 2).

An exploratory analysis comparing the six patients who developed the fibrosis endpoint with the 45 who did not identified T2DM as the strongest associated factor (100% vs. 48.9%, P = .027). Aside from T2DM, only heart failure etiology differed significantly between groups, with all fibrosis cases occurring in patients with ischemic cardiomyopathy. In this small subset, no other baseline characteristics, LVAD type, or use/duration of guideline-directed medical therapy (including SGLT2 inhibitors) showed a significant association with fibrosis status (eTable S3 in the online supplement).

Time-specific correlation analyses delineated the evolving pathophysiology (Fig. 2; full data in eTable S4). The TyG index demonstrated a striking temporal dissociation: its correlation with sST2 was absent preoperatively but became positive and sustained from 6 months post-LVAD onward (all r ≥ .594, P < .001). Conversely, its correlation with HbA1c, while significant at baseline, attenuated postoperatively (becoming non-significant at 6 months) and remained weaker. Furthermore, sST2 levels were inversely correlated with |LV-GLS| specifically at 24 months (r = − .510, P < .001), linking late-phase fibrosis to impaired systolic recovery. Exploratory analyses suggested associations between higher sST2 and lower peak VO_2 at 12–24 months, and between higher HbA1c and lower VO_2 at 6–24 months (eTable S4 in the online supplement).

DISCUSSION

In this prospective multicenter cohort of LVAD recipients, we demonstrate that pre-existing T2DM and its associated persistent insulin resistance are associated with a distinct trajectory of myocardial response to mechanical unloading. This phenotype is characterized by a sustained elevation in fibrotic stress (sST2), an attenuation of functional recovery in sensitive measures of systolic performance (LV-GLS), and a markedly increased incidence of a composite fibrosis endpoint. Critically, we emphasize that this composite endpoint, while integrating validated biomarkers of fibrotic activity, constitutes an operational definition and is not a direct histologic measure of fibrosis.

A critical consideration in interpreting our findings is that all patients exhibiting the surrogate fibrotic phenotype had established ischemic cardiomyopathy (ICM). Chronic myocardial ischemia is a well-established primary driver of maladaptive remodeling and interstitial fibrosis. Nevertheless, we emphasize that an additional—mechanistically distinct—source of myocardial fibrosis may operate in the LVAD-supported heart: mechanical unloading itself. Experimental and clinical evidence demonstrates that LVAD-induced unloading activates cardiac fibroblasts and promotes their transdifferentiation into myofibroblasts, a process independent of the underlying etiology of heart failure. Drakos et al. reported that LVAD support paradoxically increased both interstitial and total collagen content in explanted human failing hearts, concomitant with elevated microvascular density[22]. More recently, a study published in the Journal of the American Heart Association showed that myocardial fibrosis did not regress following LVAD therapy; moreover, cardiac fibroblasts isolated from HFrEF patients exhibited persistent phenotypic resistance to changes in matrix stiffness—indicating that chronic hemodynamic overload induces a durable fibroblast activation state that renders these cells insensitive to subsequent mechanical unloading[23]. This phenomenon—characterized by persistent or even progressive fibrosis after LVAD implantation, driven by sustained fibroblast activation and extracellular matrix remodeling—has emerged as a key impediment to myocardial recovery[24]. Notably, the literature remains inconsistent: while some studies report fibrosis regression post-LVAD, others document progression, and the determinants underlying these divergent trajectories remain incompletely elucidated.

Our data identify persistent insulin resistance as a potential determinant of this heterogeneity. Rather than merely reflecting a passive synergy with pre-existing ischemic scar tissue, the time-dependent emergence of the TyG–sST2 correlation during LVAD support suggests a dynamic, unloading-associated fibrotic process that is exacerbated by insulin resistance. Specifically, the TyG–sST2 correlation was absent preoperatively ($r = 0.156$, $P = 0.275$) but became statistically robust after 6 months of LVAD support ($r = 0.625$, $P < 0.001$) and further strengthened at 24 months ($r = 0.713$, $P < 0.001$; eTable S4). This temporal pattern argues against attribution solely to baseline ischemic injury—which would be expected to yield detectable correlations prior to device implantation—and instead supports an active, unloading-dependent fibrogenic mechanism. Biologically, this interpretation is reinforced by evidence demonstrating that insulin resistance directly stimulates cardiac fibroblast proliferation, enhances TGF-βsignaling, and augments collagen synthesis—thereby fostering a pro-fibrotic milieu in the diabetic and metabolically compromised myocardium [25]. Within this framework, insulin resistance may function not

only as a modifier of ischemia-driven fibrosis but also as an independent contributor to LVAD-associated fibrosis. This hypothesis merits rigorous validation in larger, prospectively enrolled cohorts—including histopathological correlation—and in patients with non-ischemic cardiomyopathies, to assess whether the association between insulin resistance and post-LVAD fibrosis extends beyond the ischemic substrate.

Our findings contribute to the growing literature on the heterogeneity of reverse remodeling. Significant interindividual variability in structural and functional recovery after LVAD support is well-established[3]. A key biological feature distinguishing “responders” from “non-responders” is the persistence of myocardial fibrosis despite mechanical unloading[4, 5]. In this context, our study provides a clinically accessible, metabolism-associated phenotype for the non-responder state: persistent insulin resistance (reflected by a sustained elevation of the TyG index) [19–21] during support is linked to rising fibrotic stress and subsequent poor functional recovery. This pattern suggests that a pre-existing and sustained state of insulin resistance may be an important factor in favorable reverse remodeling[8, 9], even when hemodynamic unloading is achieved. This association is mechanistically plausible, as insulin resistance can compromise adaptive metabolic reprogramming essential for repair. The absence of differences in LVAD operating parameters between groups underscores that the observed disparity stems from biological rather than mechanical factors.

The temporal dynamics of the association between insulin resistance and fibrotic stress is a key finding. The correlation between the TyG index and sST2 was absent preoperatively but became sustained and significant from 6 months post-LVAD onward. We propose a pathophysiological model to interpret this observation. Successful reverse remodeling requires adaptive metabolic reprogramming, for which intact insulin signaling is crucial[6, 7]. This concept is strongly supported by recent work showing that mechanical unloading activates a Hippo-YAP–INSR–pentose phosphate pathway (PPP) axis to promote myocardial repair[28]. The chronically elevated TyG index in our T2DM cohort signifies an impaired capacity for this adaptation. We hypothesize that the unmasking of the TyG-sST2 association after 6 months of support may coincide with a critical phase for attempted metabolic repair in the unloaded heart. Within the framework of the aforementioned pathway[28], persistent insulin resistance likely represents a significant impairment to this adaptive reprogramming, potentially contributing to unresolved oxidative stress and inflammation, thereby fostering a pro-fibrotic microenvironment[26]. This is reflected by the consistently higher sST2 levels in T2DM patients, providing serological data consistent with persistent myocardial stress[15, 16]. An intriguing nuance is that the TyG-sST2 correlation emerged even without a significant between-group difference in TyG at 6 months, suggesting the relationship may become more coupled during the repair phase. The dissociation between the TyG index and HbA1c postoperatively further implies that insulin resistance *Per se*—distinct from hyperglycemia—may be a more specific metabolic driver. The inverse correlation between sST2 and LV-GLS at later time points indicates that cumulative fibrotic activity may ultimately translate into detectable functional impairment[29, 30]. Existing evidence indicates that T2DM and insulin resistance are independently associated with progressive impairment of myocardial deformation, beyond conventional hemodynamic

determinants. A 7-year longitudinal study revealed that the prevalence of reduced GLS among asymptomatic individuals with T2DM increased significantly over time; multivariable analysis identified T2DM as an independent risk factor for worsening subclinical left ventricular systolic dysfunction[31]. Similarly, in patients with non-ischemic dilated cardiomyopathy, GLS was significantly lower in those with concomitant T2DM compared with those without—after adjustment for age, sex, blood pressure, and LV ejection fraction—establishing T2DM as an independent determinant of impaired GLS[32]. Critically, insulin resistance itself—not merely hyperglycemia or established diabetes—has been robustly associated with attenuated GLS values in multiple cohorts[33], and independently predicts incident subclinical left ventricular systolic dysfunction, even after rigorous control for BMI, HbA1c, fasting glucose, and traditional cardiovascular risk factors[34].We emphasize that this model remains a hypothesis-generating framework requiring further mechanistic validation.

From a translational perspective, our findings, though preliminary, highlight several considerations. First, they suggest that for T2DM patients undergoing LVAD therapy, postoperative management may warrant further investigation extending beyond glycemic control to include consideration of insulin resistance status, with the TyG index as a potential monitoring tool. Second, supported by the observed link between persistent insulin resistance and adversed remodeling, they position insulin sensitivity as a candidate pathway for therapeutic exploration to improve myocardial recovery[36, 37]. The exploratory finding that all patients meeting the fibrosis endpoint had both T2DM and ischemic cardiomyopathy suggests a potential high-risk subgroup. This observation is supported by clinical evidence linking the ACE/ACE2 axis imbalance to heightened inflammation and cardiovascular risk in diabetic patients with coronary heart disease [38], implying a shared pathophysiology that may exacerbate remodeling beyond metabolic inflexibility alone [35]. Future research should validate this phenotype in larger cohorts with histological correlation and investigate whether adjuvant therapies aimed at improving insulin sensitivity (e.g., SGLT2 inhibitors, GLP-1 receptor agonists) can modify post-LVAD remodeling trajectories[39, 40].

Study Limitations

As an exploratory observational study, our conclusions must be interpreted cautiously. A related consideration is that our non-diabetic control group included individuals receiving medications (e.g., metformin) for insulin resistance, reflecting real-world metabolic heterogeneity. While this enhances the generalizability of our findings, it may also attenuate the observed effect sizes. The sample size is limited, particularly the small number of fibrosis events, restricting robust multivariable adjustment and causal inference. The composite fibrosis endpoint is an operational definition derived from biomarker and imaging data within this cohort; while striving for clinical utility, it lacks direct histological validation. Although LVAD operating parameters were comparable, differences in medication regimens remain a potential confounding factor. Furthermore, all patients were from Chinese centers, and the generalizability of the conclusions requires validation in other populations. Several methodological limitations warrant acknowledgment. As this study constituted a retrospective analysis of prospectively collected data, original echocardiographic images and video clips were not systematically archived; only

the derived quantitative parameters were entered into the study database. Consequently, representative illustrative images could not be retrieved for inclusion in this report. Furthermore, although key methodological references have been supplemented, certain analytical techniques—including speckle-tracking echocardiography and linear mixed-effects modeling—require further standardization in future studies specifically focused on left ventricular assist devices (LVADs). Accordingly, these findings should be regarded as hypothesis-generating.

CONCLUSION

In summary, this study provides prospective clinical observations indicating an association between insulin resistance and a post-LVAD phenotype of myocardial fibrosis alongside impaired functional recovery. The underlying pathophysiology may involve insulin resistance being associated with impaired metabolic adaptations after unloading, potentially leading to sustained fibrotic signaling. The co-existence of T2DM and ICM might identify a high-risk subgroup. These findings position insulin resistance as a potential and biologically relevant factor for future investigation in the management of post-LVAD myocardial remodeling.

ABBREVIATIONS

6MWT: 6-Minute Walk Test

ACE: Angiotensin-Converting Enzyme

ACE2: Angiotensin-Converting Enzyme 2

ACEI: Angiotensin-Converting Enzyme Inhibitor

ARB: Angiotensin II Receptor Blocker

ARNI: Angiotensin Receptor-Neprilysin Inhibitor

AVOF: Aortic Valve Opening Frequency

BMI: Body Mass Index

BNP: B-Type Natriuretic Peptide

CABG: Coronary Artery Bypass Grafting

CPB: Cardiopulmonary Bypass

DCM: Dilated Cardiomyopathy

EI: Eccentricity Index

GLP-1: Glucagon-Like Peptide-1

HbA1c: Hemoglobin A1c

HFrEF: Heart Failure with Reduced Ejection Fraction

ICM: Ischemic Cardiomyopathy

ICU: Intensive Care Unit

IQR: Interquartile Range

LVAD: Left Ventricular Assist Device

LVEDd: Left Ventricular End-Diastolic Diameter

LVEF: Left Ventricular Ejection Fraction

LVESd: Left Ventricular End-Systolic Diameter

LV-GLS: Left Ventricular Global Longitudinal Strain

NETs: Neutrophil Extracellular Traps

NYHA: New York Heart Association

PCI: Percutaneous Coronary Intervention

PPP: Pentose Phosphate Pathway

RAS: Renin-Angiotensin System

RVAD: Right Ventricular Assist Device

RVFWSL: Right Ventricular Free-Wall Longitudinal Strain

SGLT2: Sodium-Glucose Cotransporter 2

sST2: Soluble Suppression of Tumorigenicity-2

T2DM: Type 2 Diabetes Mellitus

TAPSE: Tricuspid Annular Plane Systolic Excursion

TyG: Triglyceride-Glucose

VO_2 max: Maximum Oxygen Consumption

DECLARATIONS

Ethics approval and consent to participate

This study was conducted in accordance with the Declaration of Helsinki. The study protocol was approved by the Institutional Review Boards of all participating centers: Nanjing Drum Tower Hospital (Approval No.: 2024-577-02), The First Affiliated Hospital of Harbin Medical University (Approval No.: 202585), and The First Affiliated Hospital, Zhejiang University School of Medicine (Approval No.: IIT20250141B). Written informed consent was obtained from all participants or their legal guardians prior to enrollment.

Consent for publication

No applicable

Competing interests

The authors declare no competing interests.

Funding

The medical center of Nanjing cardiovascular diseases (CZLB506-2020); National Natural Science Foundation of China (82300459, 82570469, 82100289, 82200499 and 82241212).The health science and technological development foundation of Nanjing (YKK22096); Funding for clinical trial from the affiliated Drum Tower Hospital, Medical School of Nanjing University (2023-LCYJ-ZD-03).

Author Contribution

KYP, EJZ, and DHP conducted the study, contributed to statistical analysis, and drafted the manuscript. HTZ, YTL, CX and CLY participated in the study design. HLW was involved in sequence alignment. TTZ, CL, and JS performed the statistical analyses. KSL, HC, XYZ, YXX, GJX, SMW, QW, and HDP contributed to data collection. YWL, JZQ, DJW, and CLY assisted with manuscript revision. TP, JZQ, and DJW conceived the study, participated in its design and coordination, and contributed to manuscript drafting. All authors read and approved the final version of the manuscript.

Acknowledgements

During the preparation of this work, the authors used DEEPSEEK in order to revise grammatical errors. After using this tool, the authors reviewed and edited the content as needed and take full responsibility for the final content of the published article.

Data Availability

The datasets generated during and/or analyzed during the current study are available from the corresponding author on reasonable request.

REFERENCES

1. Birks EJ. Molecular changes after left ventricular assist device support for heart failure. Circ Res. 2013;113(6):777–91.
2. Shah P, Psotka M, Taleb I, Alharethi R, Shams MA, Wever-Pinzon O, Yin M, Latta F, Stehlik J, Fang JC, Diao G, Singh R, Ijaz N, Kyriakopoulos CP, Zhu W, May CW, Cooper LB, Desai SS, Selzman CH, Kfoury AG, Drakos SG. Framework to classify reverse cardiac remodeling with mechanical circulatory support: the utah-inova stages. Circ Heart Fail. 2021;14(5):e007991.
3. Lu Y, Zhao S, Han J, Lv Q, Du X, Hua Z, Huang K, Ge Z, Sun X, Zhu D, Shao Y, Zhang H, Gong M. Multicenter study for CH-VAD as a fully magnetically levitated left ventricular assist device. iScience. 2025;28(2):111764.
4. Castillero E, Ali ZA, Akashi H, Giangreco N, Wang C, Stöhr EJ, Ji R, Zhang X, Kheysin N, Park JS, Hegde S, Patel S, Stein S, Cuenca C, Leung D, Homma S, Tatonetti NP, Topkara VK, Takeda K, Colombo PC, Naka Y, Sweeney HL, Schulze PC, George I. Structural and functional cardiac profile after prolonged duration of mechanical unloading: potential implications for myocardial recovery. Am J Physiol Heart Circ Physiol. 2018;315(5):H1463–76.
5. Birks EJ. Molecular changes after left ventricular assist device support for heart failure. Circ Res. 2013;113(6):777–91.
6. Badolia R, Ramadurai DKA, Abel ED, Ferrin P, Taleb I, Shankar TS, Navankasattusas S, McKellar SH, Wever-Pinzon O, Ling Y, Yin M, Kfoury AG, Greene T, Drakos SG. The role of nonglycolytic glucose metabolism in myocardial recovery upon mechanical unloading and circulatory support in chronic heart failure. Circulation. 2020;142(3):259–74.
7. Drakos SG, Badolia R, Makaju A, Kyriakopoulos CP, Wever-Pinzon O, Tracy CM, Abel ED, Taleb I, Yin M, Shankar TS, Navankasattusas S, Ramadurai DKA, McKellar SH, Greene T. Distinct transcriptomic and proteomic profile specifies patients who have heart failure with potential of myocardial recovery on mechanical unloading and circulatory support. Circulation. 2023;147(5):409–24.
8. Kyriakopoulos CP, Taleb I, Tseliou E, Sideris K, Hamouche R, Maneta E, Nelson M, Krauspe E, Selko S, Dranow E, Goodwin ML, Alharethi R, Wever-Pinzon O, Fang JC, Stehlik J, Selzman CH, Hanff TC, Drakos SG, Visker JR. Impact of diabetes and glycemia on cardiac improvement and adverse events following mechanical circulatory support. J Am Heart Assoc. 2024;13(14):e032936.
9. Bellemare M, Bourcier L, Iglesies-Grau J, Boulet J, O'Meara E, Bouabdallaoui N. Mechanisms of diabetic cardiomyopathy: focus on inflammation. Diabetes Obes Metab. 2025;27(5):2326–38.
10. Karimi F, Maleki M, Movahedpour A, Alizadeh M, Kharazinejad E, Sabaghan M. Overview of the renin-angiotensin system in diabetic nephropathy. J Renin Angiotensin Aldosterone Syst. 2024;25.

11. Kanwar MK, Selzman CH, Ton VK, Miera O, Cornwell WK 3rd, Antaki J, Drakos S, Shah P. Clinical myocardial recovery in advanced heart failure with long term left ventricular assist device support. J Heart Lung Transpl. 2022;41(10):1324–34.
12. Burkhoff D, Topkara VK, Sayer G, Uriel N. Reverse remodeling with left ventricular assist devices. Circ Res. 2021;128(10):1594–612.
13. Lang RM, Badano LP, Mor-Avi V, Afilalo J, Armstrong A, Ernande L, Flachskampf FA, Foster E, Goldstein SA, Kuznetsova T, Lancellotti P, Muraru D, Picard MH, Rietzschel ER, Rudski L, Spencer KT, Tsang W, Voigt JU. Recommendations for cardiac chamber quantification by echocardiography in adults: an update from the American Society of Echocardiography and the European Association of Cardiovascular Imaging. J Am Soc Echocardiogr. 2015;28(1):1–e3914.
14. Simental-Mendía LE, Rodríguez-Morán M, Guerrero-Romero F. The product of fasting glucose and triglycerides as surrogate for identifying insulin resistance in apparently healthy subjects. Metab Syndr Relat Disord. 2008;6(4):299–304.
15. Arrieta V, Jover E, Navarro A, Martín-Núñez E, Garaikoetxea M, Matilla L, García-Peña A, Fernández-Celis A, Gainza A, Álvarez V, Sádaba R, López-Andrés N. Soluble ST2 levels are related to replacement myocardial fibrosis in severe aortic stenosis. Rev Esp Cardiol (Engl Ed). 2023;76(9):679–89.
16. Tseng CCS, Huibers MMH, Gaykema LH, Siera-de Koning E, Ramjankhan FZ, Maisel AS, de Jonge N. Soluble ST2 in end-stage heart failure, before and after support with a left ventricular assist device. Eur J Clin Invest. 2018;48(3):e12886.
17. Thomas JD, Edvardsen T, Abraham T, Appadurai V, Badano L, Banchs J, Cohen-Solal A, Cotrim C, Devereux RB, Flachskampf FA, Galderisi M, Haugaa KH, Khanji MY, Manka R, Mousavi N, Pedrizzetti G, Plonska-Gosciniak E, Smiseth OA, Voigt JU, Zoghbi WA. Clinical applications of strain echocardiography: a clinical consensus statement from the American Society of Echocardiography developed in collaboration with the European Association of Cardiovascular Imaging of the European Society of Cardiology. J Am Soc Echocardiogr. 2025;38(11):985–1020.
18. Fitzmaurice GM, Laird NM, Ware JH. Applied longitudinal analysis. 2nd ed. Hoboken: Wiley; 2011.
19. Zhou H, Ding X, Lan Y, Chen S, Wu S, Wu D. Multi-trajectories of triglyceride-glucose index and lifestyle with cardiovascular disease: a cohort study. Cardiovasc Diabetol. 2023;22(1):341.
20. Lopez-Jaramillo P, Gomez-Arbelaez D, Martinez-Bello D, Abat MEM, Alhabib KF, Avezum Á, Barbarash O, Chifamba J, Diaz R, Gupta R, Iqbal R, Kelishadi R, Khatib R, Lanas F, Lear SA, Li W, Liu L, Lopez-Lopez JP, Masoudi FA, Mony PK, Oguz A, Palileo-Villanueva LM, Perez-Mayorga M, Poirier P, Rangarajan S, Rosengren A, Soman SS, Swaminathan S, Teo K, Wielgosz A, Yusufali A, Yusuf S. Association of the triglyceride glucose index as a measure of insulin resistance with mortality and cardiovascular disease in populations from five continents (PURE study): a prospective cohort study. Lancet Healthy Longev. 2023;4(1):e23–33.
21. Khalaji A, Behnoush AH, Khanmohammadi S, Ghanbari Mardasi K, Sharifkashani S, Sahebkar A, Vinciguerra C, Cannavo A. Triglyceride-glucose index and heart failure: a systematic review and

meta-analysis. Cardiovasc Diabetol. 2023;22(1):244.

22. Drakos SG, Kfoury AG, Hammond EH, Reid BB, Revelo MP, Rasmusson BY, Whitehead KJ, Salama ME, Selzman CH, Stehlik J, Clayson SE, Bristow MR, Renlund DG, Li DY. Impact of mechanical unloading on microvasculature and associated central remodeling features of the failing human heart. J Am Coll Cardiol. 2010;56(5):382–91.
23. Biggs RM, Zhang Y, Silverman DN. Persistent fibrosis in heart failure with a reduced ejection fraction linked to phenotypic differences in human cardiac fibroblast populations. J Am Heart Assoc. 2025;14(8):e039747.
24. Natarajan K, Krishnamoorthi MK, Palaniyandi SS, Watanabe K, Pownall HJ, Guha A, Bhimaraj A, Thandavarayan RA. Therapeutic strategies for reversing cardiac fibrosis in hearts supported by ventricular assist devices. Drug Discov Today. 2025;30(12):104547.
25. Tuleta I, Frangogiannis NG. Fibrosis of the diabetic heart: clinical significance, molecular mechanisms, and therapeutic opportunities. Adv Drug Deliv Rev. 2021;176:113904.
26. Chen W, Frangogiannis NG. The role of inflammatory and fibrogenic pathways in heart failure associated with aging. Heart Fail Rev. 2010;15(5):415–22.
27. Cheng J, Huang Y, Zhang X, Yu Y, Wu S, Jiao J, Huang K, Zhang L, Chen Z. TRIM21 and PHLDA3 negatively regulate the crosstalk between the PI3K/AKT pathway and PPP metabolism. Nat Commun. 2020;11(1):1880.
28. Pan T, Liu T, Jiang C, Yu X, Ji Y, Liu J, Zhang H, Han X, Jiang X, Li Y, Qu JZ, Dong J, Wang DJ. Insulin resistance compromises the pentose phosphate pathway and impairs left ventricular assist device-mediated myocardial recovery in obese patients with heart failure. Circulation. 2026;153:1141–64.
29. Toro S, Patel K, Guha A. Destination LVAD therapy in the current era of the heart transplant allocation system. Curr Opin Cardiol. 2023;38(3):275.
30. Tseliou E, Lavine KJ, Wever-Pinzon O, Topkara VK, Meyns B, Adachi I, Zimpfer D, Birks EJ, Burkhoff D, Drakos SG. Biology of myocardial recovery in advanced heart failure with long-term mechanical support. J Heart Lung Transpl. 2022;41(10):1309–23.
31. Akasheva DU, Utina TG, Dzhioeva ON, Drapkina OM. Subclinical left ventricular dysfunction over seven-year follow-up in type 2 diabetes patients without cardiovascular diseases. Biomedicines. 2024;12(9):2031.
32. Tanaka H, Tatsumi K, Matsuzoe H, Matsumoto K, Hirata KI. Impact of diabetes mellitus on left ventricular longitudinal function of patients with non-ischemic dilated cardiomyopathy. Cardiovasc Diabetol. 2020;19:84.
33. Elenizi K, Alharthi R, Alanazi A, Alotaibi N, Alajmi M, Alsubaie A, Gamil S, Alqahtani M. Impact of uncontrolled diabetes on myocardial global longitudinal strain: a case-control study. Rev Cardiovasc Med. 2025;26(6):38967.
34. Atici A, Asoglu R, Barman HA, Sarikaya R, Arman Y, Tukek T. Multilayer global longitudinal strain assessment of subclinical myocardial dysfunction related to insulin resistance. Int J Cardiovasc Imaging. 2021;37(2):539–46.

35. Nakamura M, Sadoshima J. Cardiomyopathy in obesity, insulin resistance and diabetes. J Physiol. 2020;598(14):2977–93.
36. Heshmat A, Wakeel LME, Khorshid H, Fahmy SF. Impact of dapagliflozin administration on remodeling marker and clinical outcomes of STEMI patients with diabetes mellitus: a controlled clinical trial. Futur J Pharm Sci. 2025;11:106.
37. Albulushi A, Askari KM, Al-Abedi AM, Al-Kulaibi MA, Hasan MS, Hosseini Z, Al-Rahman MT, Tanoh DB, Hasan AS, Al-Helli Y, Basouni A. Impact of SGLT2 inhibitors on myocardial fibrosis in diabetic HFpEF: a longitudinal study. Eur J Med Res. 2025;30(1):592.
38. Naveena G, Shivasekar M, Vinodhini VM, Kumar JS. Association of ACE & ACE2 with inflammatory markers studied in T2DM patients with & without CHD. J Renin Angiotensin Aldosterone Syst. 2025;26.
39. Bell DSH, Jerkins T. In praise of pioglitazone: an economically efficacious therapy for type 2 diabetes and other manifestations of the metabolic syndrome. Diabetes Obes Metab. 2023;25(11):3093–102.
40. DeFronzo RA, Inzucchi S, Abdul-Ghani M, Nissen SE. Pioglitazone: the forgotten, cost-effective cardioprotective drug for type 2 diabetes. Diab Vasc Dis Res. 2019;16(2):133–43.

TABLES

Table 1: Baseline characteristics

Variables	Total (n=54)	Control Group (N=26)	T2DM Group (n=28)	P Value
Age (year)	61.50(50.00-67.25)	61.00(46.20-65.25)	62.00(54.00-68.75)	.176
Gender (male, %)	50,92.59%	24,92.30%	26,92.58%	.939
BMI (kg/m^2)	23.46(22.11-25.24)	23.47(22.05-25.14)	23.46(22.49-26.31)	.842
NYHA ≥ III	41,75.92%	21,80.76%	20,71.42%	.422
Etiology (n, %)				.151
DCM	32,59.26%	18,69.23%	14,50%	
ICM	22,40.74%	8,30.76%	14,50%	
Medical History (n, %)				
Atrial fibrillation	11,20.3%	3,11.53%	8,28.57%	.120
Hypertension	26,48.15%	10,38.46%	16,57.14%	.170
Critical preoperative condition[a]	14,25.92%	9,34.61%	5,17.85%	.160
Pulmonary hypertension	12,22.22%	4,15.38%	8,28.57%	.244
Kidney dysfunction	13,24.07%	6,23.07%	7,25.00%	.869
Liver dysfunction	4,7.40%	3,11.53%	1,3.57%	.264
Autoimmune diseases	4,7.40%	3,11.53%	1,3.57%	.264
Prior cardiac surgery	0	0	0	—
Prior non-cardiac surgery	5,9.25%	4,15.38%	1,3.57%	.135
PCI	10,18.51%	3,11.53%	7,25.00%	.203
Pre-op medications (n, %)				
Inotrope dependence	47,87.03%	23,88.46%	24,85.71%	.764
Beta-blocker	48,88.88%	23,88.46%	25,89.25%	.923
ACEI/ARB/ARNI	44,81.48%	20,76.92%	24,85.71%	.406
Mineralocorticoid antagonist	44,81.48%	20,76.92%	24,85.71%	.406

Therapeutic anticoagulation	34,62.96%	15,57.69%	19,67.85%	.440
Aspirin	43,79.62%	20,76.92%	23,82.14%	.634
Diuretics	44,81.48%	20,76.92%	24,85.71%	.406
SGLT2 inhibitor	23,42.59%	4,15.38%	19,67.85%	<.001
GLP-1 agonist	8,14.81%	3,11.53%	5,17.85%	.514
Insulin	30,55.55%	2,7.69%	28,100%	<.001
Metformin	24,44.44%	1,3.84%	23,82.14%	<.001
LVAD type (n, %)				
EVAHEART	6,11.11%	4,15.38%	2,7.14%	.738
HEART-Con	13,24.07%	3,11.53%	10,35.71%	
Brio-HEART	3,5.55%	3,11.53%	0	
Cor-HEART 6	32,59.25%	16,61.53%	16,57.14%	
Combined procedure (n, %)				.633
None	11,20.37%	7,26.92%	4,14.28%	
CABG +/- LVAR	18,33.33%	7,26.92%	11,39.28%	
Valve repair	25,46.29%	12,46.15%	13,46.42%	
CPB time (minutes)	162(142-189)	161(136-215)	165(144-187)	.683
ACC time (minutes)	115(98-122)	115(95-136)	115(99-122)	.903

CABG: Coronary artery bypass grafting

BMI: Body mass index

LVEF: Left ventricular ejection fraction

LVAR: Left Ventricular Aneurysm Repair

DCM: Dilated cardiomyopathy

ICM: Ischemic cardiomyopathy

PCI: Percutaneous coronary intervention

Pre-op: preoperative

CPB: Cardiopulmonary bypass

ACC: Aortic cross-clamp

ACEI: Angiotensin-converting enzyme inhibitor

ARB: Angiotensin II receptor blocker

ARNI: Angiotensin receptor–neprilysin inhibitor

SGL2: Sodium-glucose cotransporter 2

GLP-1: Glucagon-like peptide-1

a: Critical Preoperative Condition was defined as the presence of one or more of the following: preoperative extracorporeal membrane oxygenation (ECMO) support, intra-aortic balloon pump (IABP) support, or refractory cardiogenic shock.

Table 2: Postoperative and follow-up outcomes

Outcomes	Total (n=54)	Control Group (N=26)	T2DM Group (n=28)	P Value
In hospital (n, %)				
MV time (hours)	18(16-22)	17.50(15.75-21.00)	18.50(17.50-24.25)	.077
ICU time (days)	7(5-11)	6(5-13)	7(5-11)	.171
Renal replacement therapy	21,38.89%	7,26.92%	14,50%	.082
Reoperation for bleeding	4,7.41%	3,11.53%	1,3.57%	.264
Stroke	1,1.85%	1,3.84%	0	.295
Driveline infection	3,5.55%	2,7.69%	1,3.57%	.509
Sepsis	1,1.85%	1,3.84%	0	.295
Mortality	2,3.70%	2,7.69%	0	.135
Follow-up (n, %)				
Follow-up time (months) [a]	24(20-24)	22(18-25)	24(22-25)	.121
Survival at 30 days [a]	51, 98.08%	23, 95.83%	28, 100%	.172
Survival at 1 year[b]	51, 100%	23, 100%	28, 100%	.172
Overall survival[b]	51, 100%	23, 100%	28, 100%	.172
Stroke[b]	2, 3.92%	0	2,7.14%	.182
LVAD related infection[b]	5, 9.80%	1, 4.35%	4,14.28%	.201
Gastrointestinal bleeding[b]	7, 13.72%	1, 4.35%	6,21.42%	.069
Heart failure re-admission[b]	16, 31.37%	4 ,17.39%	12,42.85%	.041
Myocardial fibrosis[b]	6, 11.76%	0	6,21.42%	.018
Follow-up medications(n, %)[b]				
SGLT2	27, 52.94%	8, 34.78%	19,67.85%	.009
Duration of therapy (months)	13.50(12.60-16.00)	12.50(12.00-15.50)	14.00(13.00-16.00)	.004
ACEI/ARB/ARNI	44, 86.27%	19, 82.61%	25,89.28%	.198

Duration of therapy (months)	19.00(15.00-21.00)	15.00(14.50-17.10)	20.00(18.50-21.00)	.003
Mineralocorticoid antagonist	46, 90.20%	20, 86.96%	26,92.85%	.168
Duration of therapy (months)	20.00(14.00-22.00)	14.00(13.00-18.00)	20.00(19.00-22.00)	.444
Beta-blocker	41, 80.39%	18, 78.26%	23,82.14%	.378
Duration of therapy (months)	16.00(13.00-19.00)	14.50(12.00-18.50)	17.00(12.00-20.00)	.152
Antihyperglycemic therapy	33, 64.71%	3, 13.04%	28,100%	<.001
Duration of therapy (months)	22.00(20.00-22.50)	1.00(1.00-1.50)	22.00(20.50-23.00)	<.001

MV: Mechanical ventilation

ICU: Intensive care unit

ACC: Aortic cross-clamp

ACEI: Angiotensin-converting enzyme inhibitor

ARB: Angiotensin II receptor blocker

ARNI: Angiotensin receptor–neprilysin inhibitor

SGL2: Sodium-glucose cotransporter 2

GLP-1: Glucagon-like peptide-1

a: Two patients died during the index hospitalization in the control group, leaving 52 patients for serial follow-up evaluation

b: In the control group, two patients died during the index hospitalization, and one patient died within 30 days after discharge, leaving 51 patients for serial follow-up evaluation

Figures

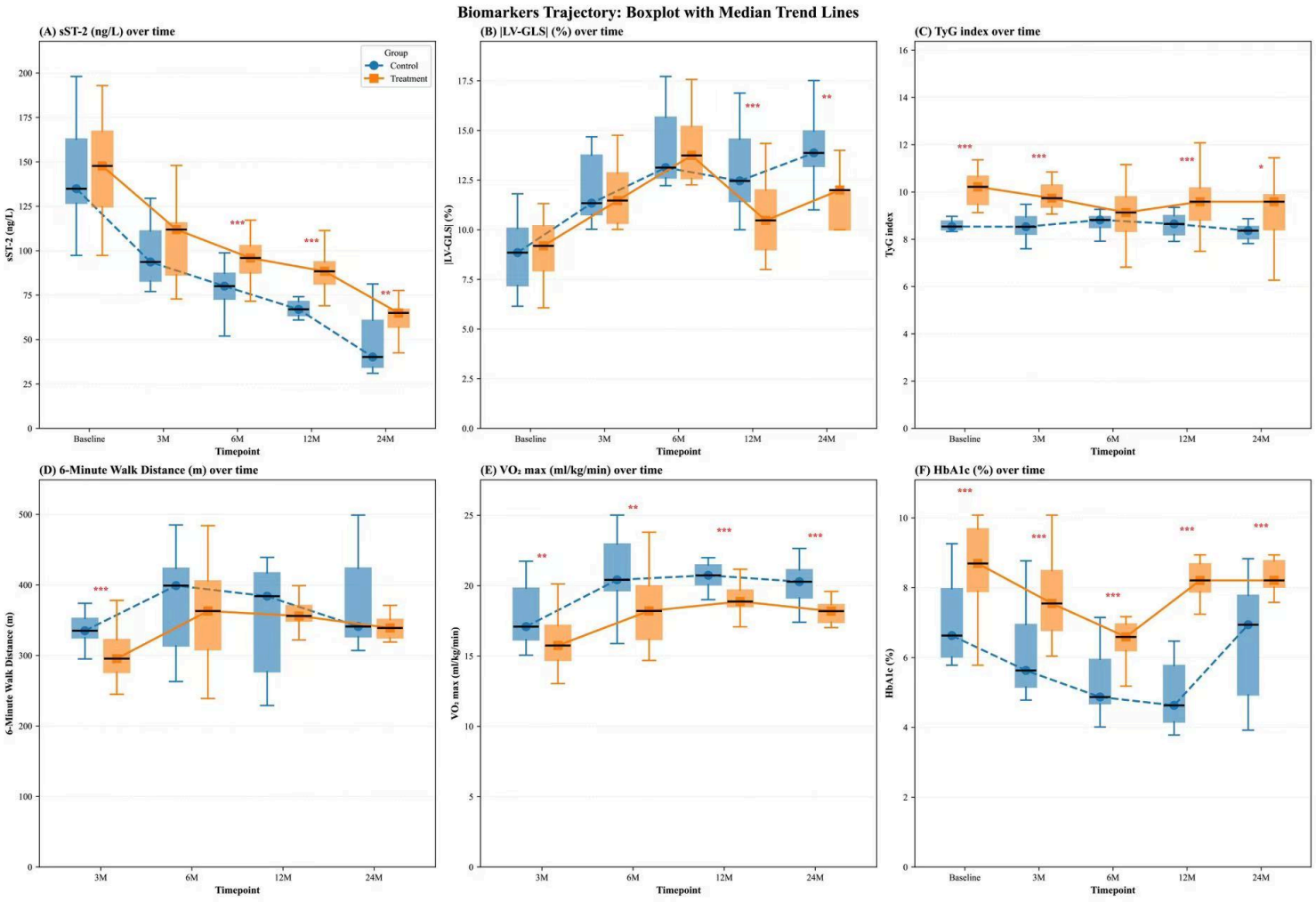


Figure 1

Longitudinal trajectories of fibrosis biomarker, systolic function, functional capacity, cardiac structure, and glycemic control after LVAD implantation, stratified by type 2 diabetes mellitus (T2DM) status.
A: sST2 levels were persistently higher in T2DM patients from 6 months onward (time and group $P <$ .001; interaction P = .048).
B: |LV-GLS| was worse in the T2DM group from 12 months onward (time $P <$ .001).
C: TyG index remained higher in T2DM patients throughout follow-up (group $P <$ .001; interaction P = .245).
D: 6MWT distance was lower in the T2DM group (group P = .043).
E: VO_2 max was consistently lower in T2DM patients (group P = .013).
F: HbA1c remained higher in the T2DM group (group $P <$ .001).

Data are presented as median with interquartile range. *P < .05, **P < .01, *P < .001 for between-group comparisons at individual time points (these P values were not adjusted for multiple comparisons). The P values reported in the panel descriptions are from linear mixed-effects models. T2DM, type 2 diabetes mellitus.

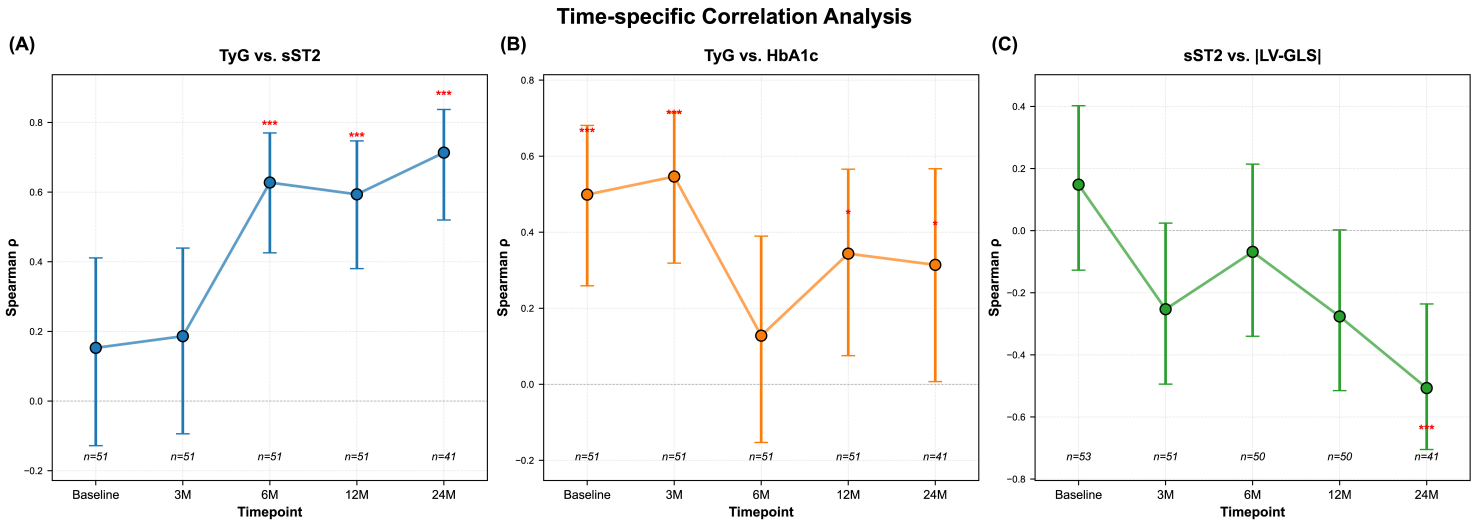


Figure 2

Time-specific correlation analyses.

Dynamic evolution of correlation coefficients for key variable pairs across the study timeline: Triglyceride-Glucose index (TyG) versus soluble suppression of tumorigenicity-2 (sST2) (blue line), TyG versus glycated hemoglobin (HbA1c) (orange line), and sST2 versus absolute left ventricular global longitudinal strain (|LV-GLS|) (green line). *P < .05, **P < .01, *P < .001

Supplementary Files

This is a list of supplementary files associated with this preprint. Click to download.

- eTableS1.docx